Supplementary Figure document for Cooper et al 2026., "Tau toxicity is gated through the ^{306}VQIVYK^{311} domain but through mechanisms not entirely dependent on Tau aggregation".

Supplementary Figure 1. Tau is equally expressed by all mutants.

(A) Western immunoblot analysis of total Tau (α-hTau Dako), taken from 15 male, 2 day old homogenised transgenic fly heads expressing wildtype mCherry::hTau2N4R and mutant forms. Driver is GMR.ninaE-GAL4. Representative blot is shown (**A**) and mean quantification plotted as a bar graph (**A'**) (n=3 biological repeats). Error bars presented as means with SEM. β-actin was used as the loading control. mCherry::hTau constructs each run at ~100kDa due to the extra weight of the fluorescent tag (hTau2N4R usually runs at ~70kDa) and Actin runs between 35 and 55kDa, at ~45kDa.

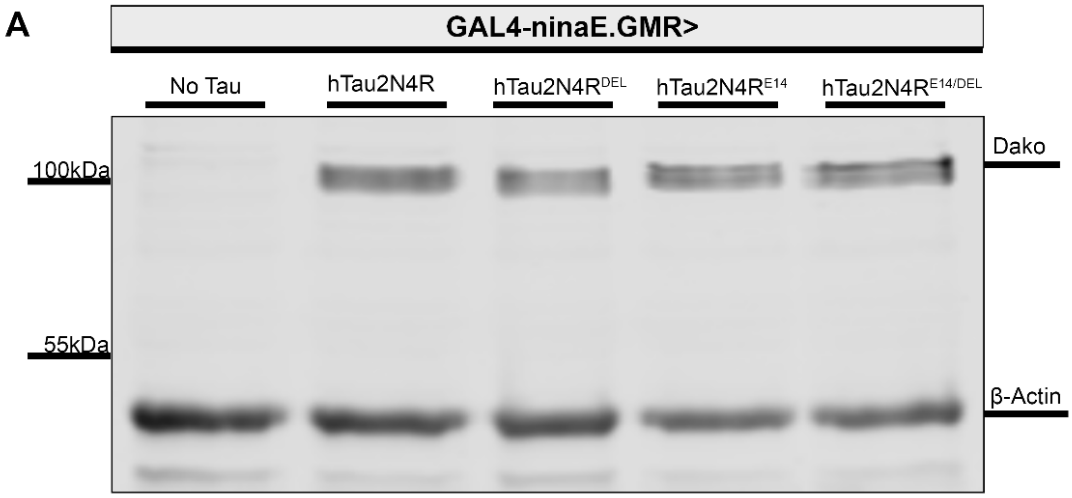

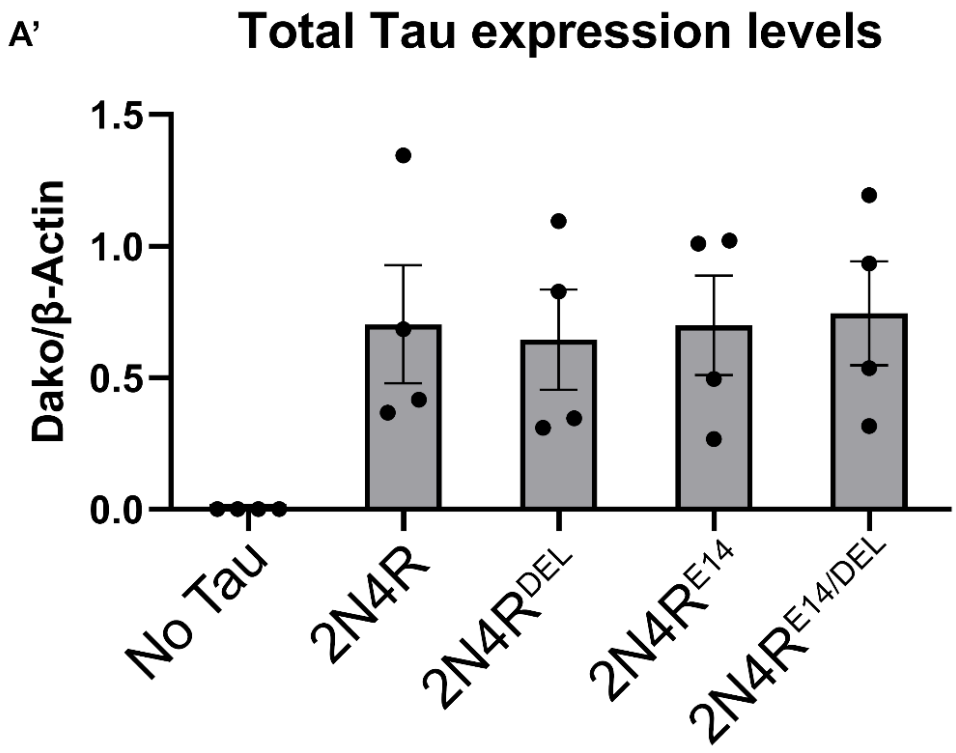

Supplementary Figure 2. The Or47b expressing olfactory sensory neurons.

Panel A. Schematic panel orientation of the adult *Drosophila* brain, showing the location of the olfactory receptor 47b (Or47b) neurons expressing membrane bound GFP (green), co-expressing mCherry tagged human Tau2N4R (mCh::hTau) (magenta). Representative confocal images of whole mount (**A**) Antenna and (**C**) the Antennal lobe (AL) is shown. (**B**) Schematic diagram of the Or47b olfactory neurons. The AL is outlined in dashed black, containing multiple olfactory glomeruli, including Or47b (green) containing a bundle of ~60 olfactory receptor neurons (ORNs). ORN cell bodies are contained within the 3rd antennal segment of the Antenna (**A, A'**) and its dendrite projects into the sensilla hairs of the antenna. The axons project from the antenna connecting into the (**C**) AL of the brain, containing the (**C'**) axonal bundles and synaptic terminals of the Or47b neuron. For simplicity, only a few of the 60 ORNs are shown.

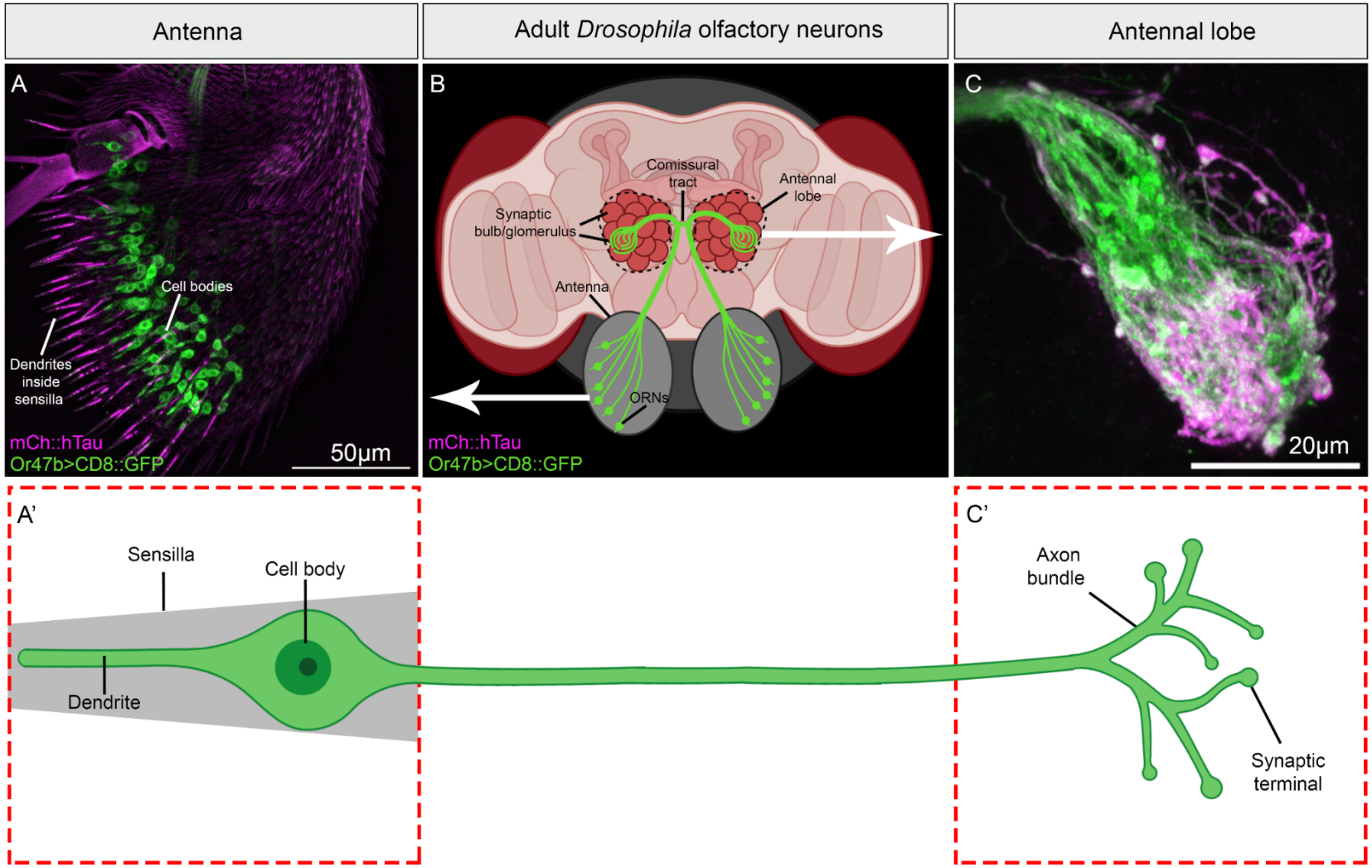

Supplementary Figure 3. T3 Axonal degeneration and Tau accumulation.

(A) Maximum projection confocal images of the adult antenna of flies expressing membrane bound GFP (CD8::GFP) at the Or47b neurons at day 3. Columns represent genotypes expressing different mCherry-tagged hTau2N4R variants plus the driver GFP only control (left most column). (**B**) Maximum projection confocal (**B1-5**) images of the brain, antennal lobe of day 3 old flies expressing mCherry::Tau mutants in the Or47b neurons (enhanced with α-hTau Dako). Arrows point toward beaded Tau accumulates.

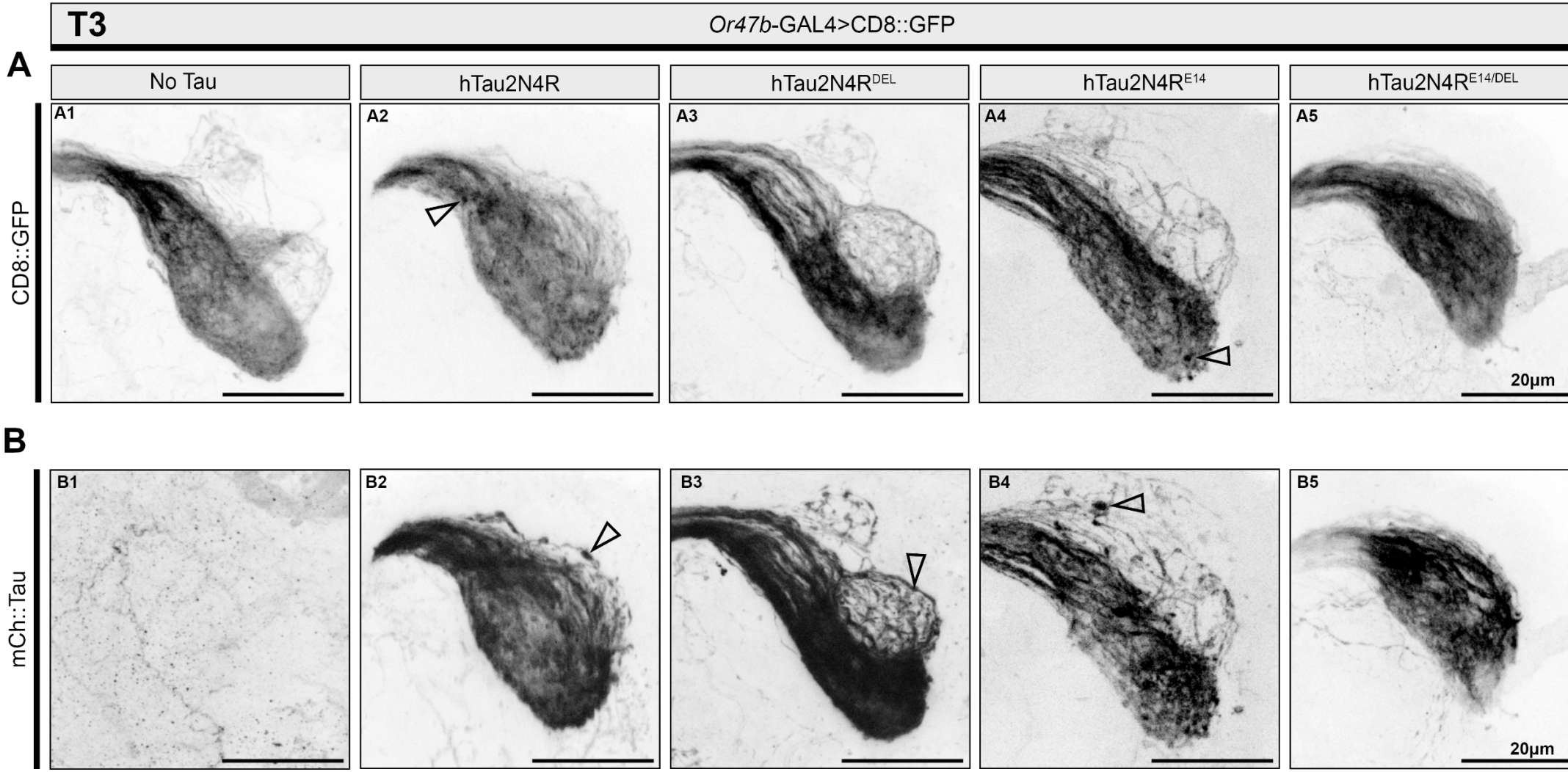

Supplementary Figure 4. Total volume of GFP expressing neurons. Quantification of neuron volume was automatically quantified using 3D images with IMARIS (see methods). Graphs represent mean ±SD, and dots represent individual values. * = $p<0.05$ (2-way ANOVA with Tukey's multiple comparisons). N= 6-14 brains collected from two biological repeats per genotype.

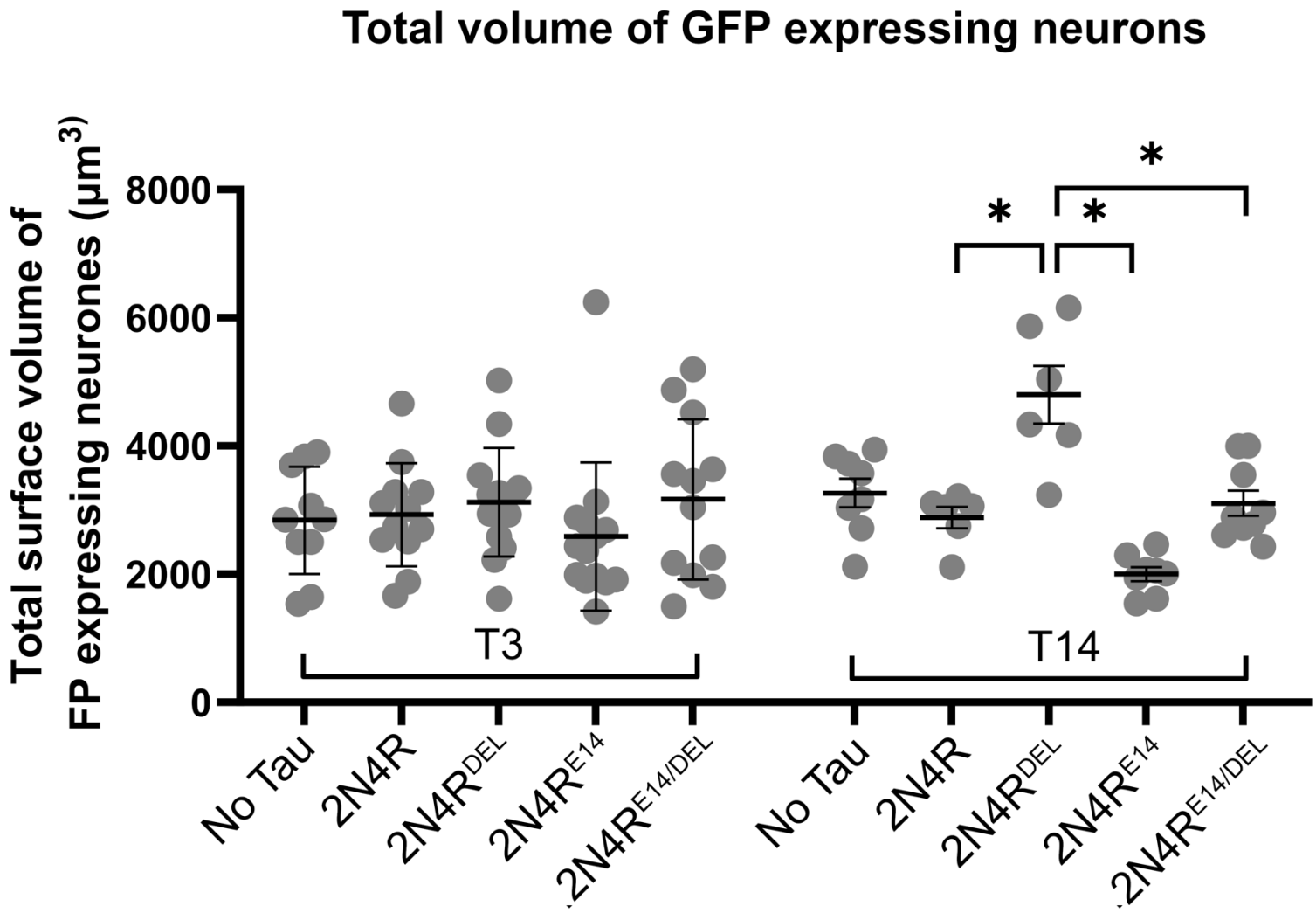

Supplementary Figure 5. *Drosophila* eye diagram, phosphorylation dependent retinal degeneration requires aggregation.

(**A**) SEM micrograph of whole *Drosophila* head. White insert shows the posterior region of interest where Tau-mediated retinal degeneration occurs using the GAL4-ninaE.GMR driver. (**A'**) The *Drosophila* eye comprises of ~800 single ommatidia units (highlighted in yellow) which are morphologically sensitive to toxic proteins like Tau. Loss of sensory bristles (blue arrows) are also markers of retinal health, which are viewed using SEM techniques. (**B**) Digital microscope images (600x) of *Drosophila* eyes expressing each hTau2N4R mutant. A rough appearance of the posterior half of the eye appears after hTau2N4R expression (**B2)** and is exacerbated by the TauE14 mutations (**B4).**

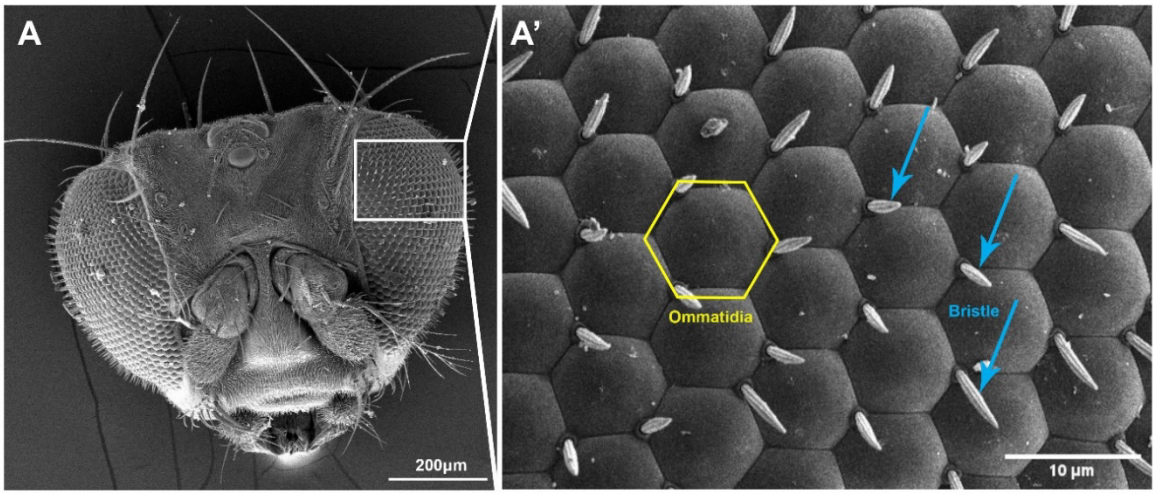

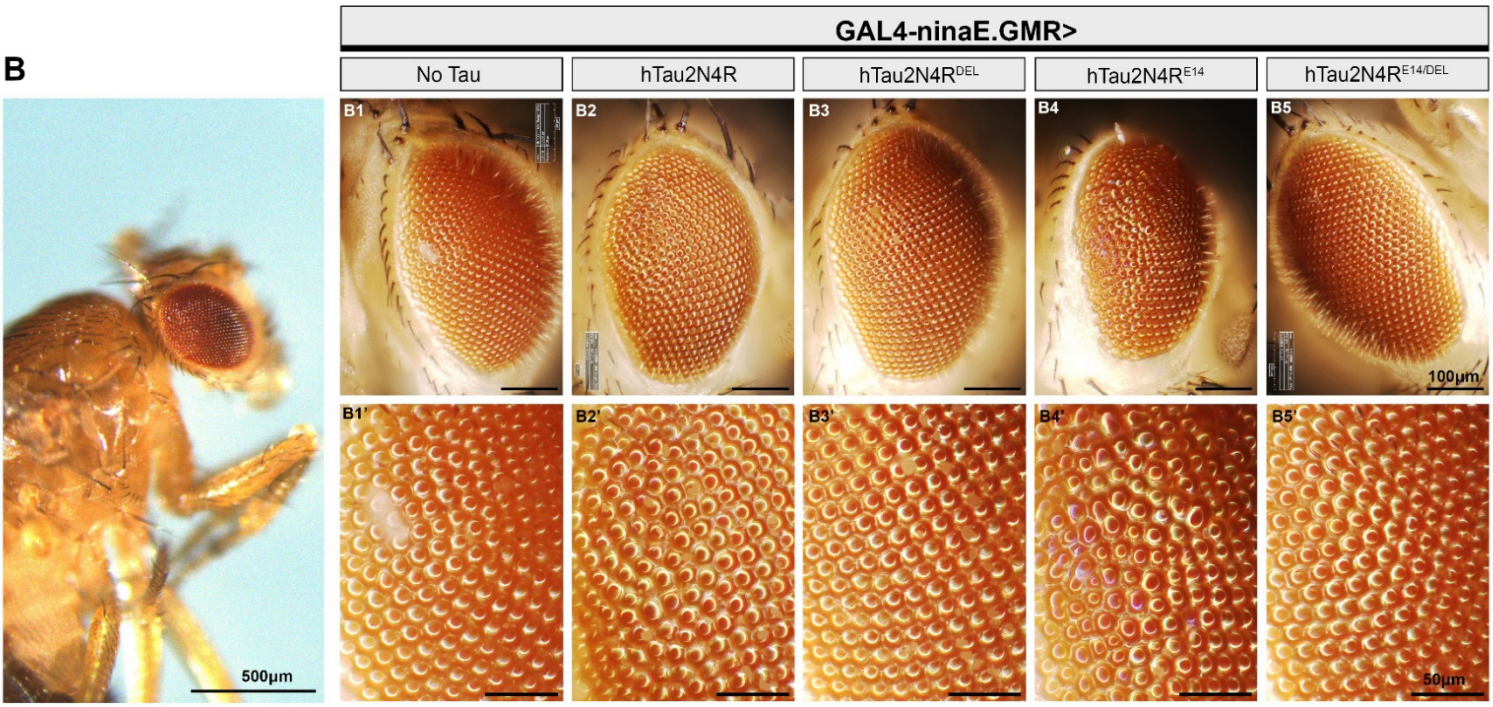

Supplementary Figure 6. T3 and T14 somato-dendritic Tau accumulation in whole mount antenna.

Midline 30 slice stacked confocal images of the adult antenna of flies labelled by the mCherryTau signal from expressed mutants in the Or47b neurons. Columns represent genotypes expressing different mCherry-tagged hTau2N4R variants plus the driver GFP only control (left most column). Rows represent post-developmental age 3 or 14 days.

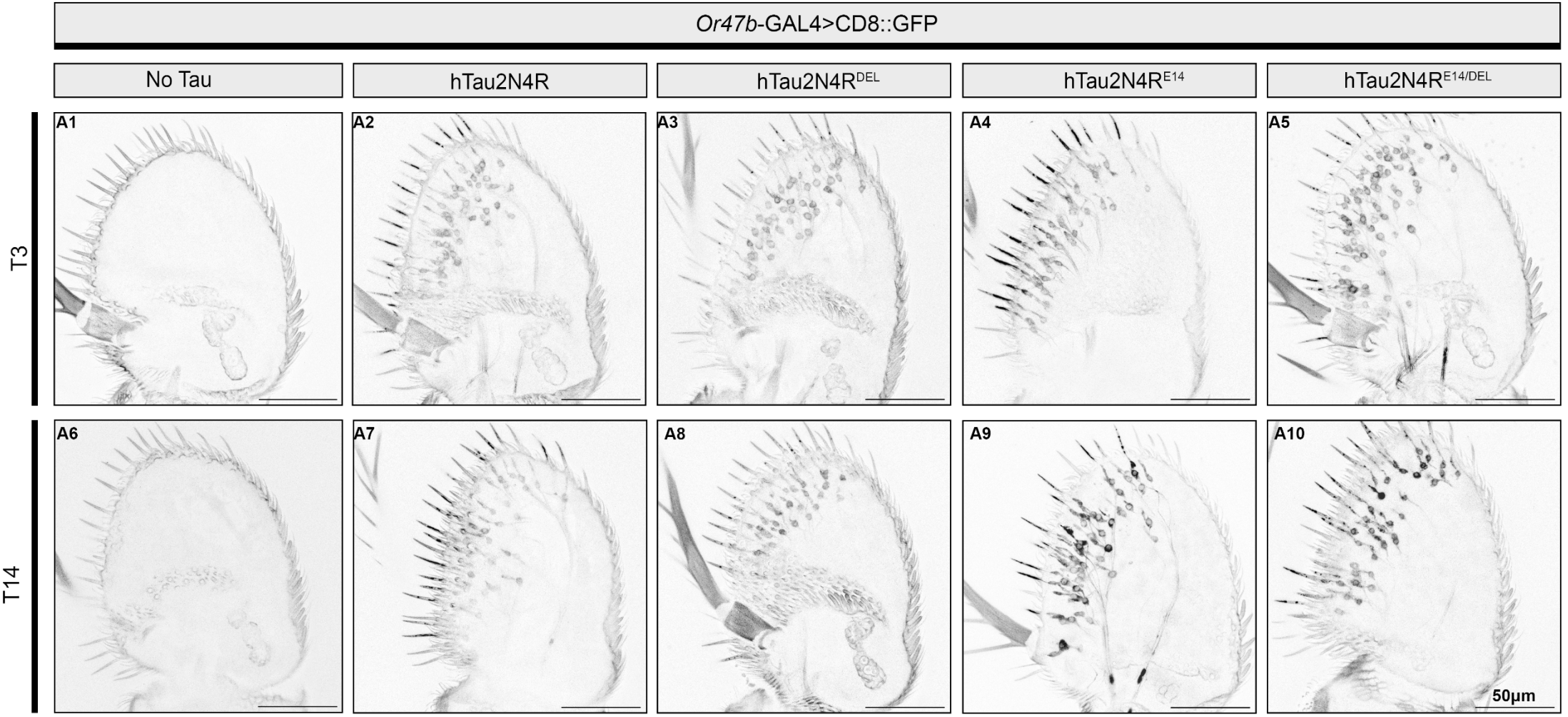

Supplementary Figure 7. Aqueous soluble, sarkosyl-soluble and sarkosyl-insoluble fractions isolated from transgenic *Drosophila* brain homogenates.

Comparison of aqueous soluble monomeric Tau (S1), sarkosyl soluble, oligomeric Tau (S2) and sarkosyl insoluble, fibrillar Tau(S3) and enriched fractions between **A)** hTau2N4R vs hTau2N4R^{DEL} and **B)** hTau2N4R^{E14} vs hTau2N4R$^{E14/DEL}$ expressing flies tested after 14 days of aging. Driver used was GAL4-GMR.ninaE. Genetic crosses set up at 25°C and progeny aged at 29°C (n=164 heads 50:50 male:female). (A-B) Representative Western blots probed with anti-hTau (Dako) comparing Tau fractions. mCherry-tagged Tau constructs migrate at ~100 kDa.

C) Quantitative analysis the relative distribution of all Tau fractions. Equal volumes were loaded for all fractions. Tau signal was scaled to account for differences in fraction volume prior to normalisation, reflecting concentration of the Sarkosyl insoluble fraction. Scaled values were expressed as a proportion of the sum total Tau of all three fractions. Eg. S1/(S1+S2+S3). No significant differences were observed between genotypes in any fraction or ratio analysed. Graphs represent mean ±SD (N=3 biological replicates). Statistical analysis performed was a one-way ANOVA.

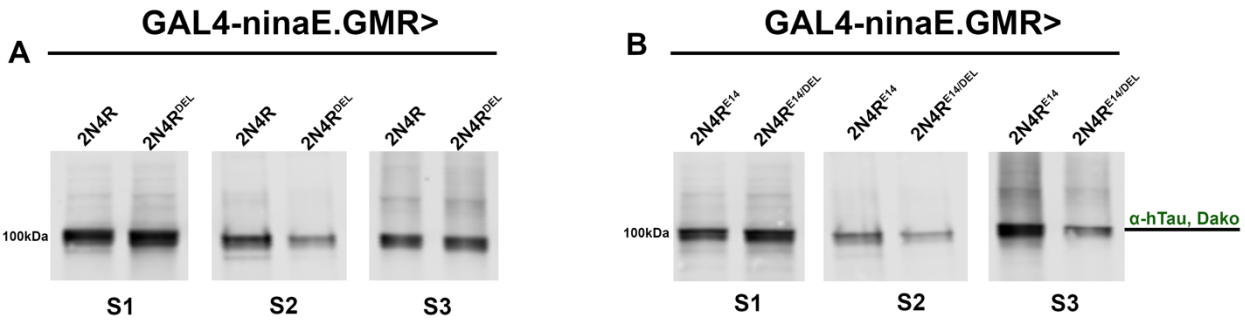

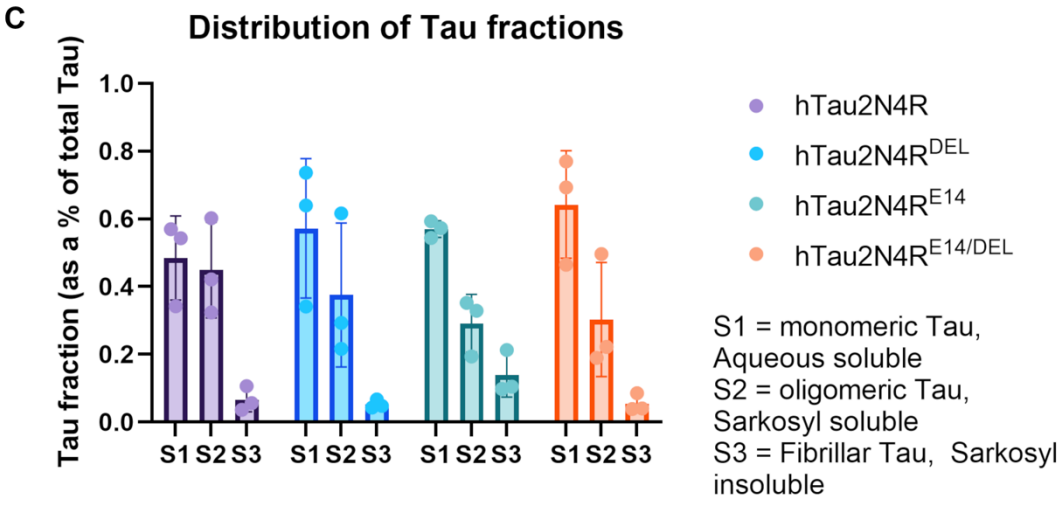

Supplementary Figure 8. Aggregation inhibition does not alter p-Tau expression at multiple Alzheimer's disease relevant sites in aged hTau2N4R expressing *Drosophila*.

Western immunoblot analysis and quantification of (**A)** total Tau (a-hTau Dako) and p-Tau expression at AT8 (Ser202,Thr205), AT180 (Thr231), AT270 (Thr181), PHF-1(Ser396, Ser404) and Ser262 epitopes did not significantly change between 14 day old transgenic flies expressing WT hTau2N4R and hTau2N4R^{DEL}. Error bars presented as means ± SEM. Driver is GMR.ninaE-GAL4. (**A')** Representative blot is shown. β-actin was used as the loading control. mCherry::hTau2N4R constructs each run around 100kDa due to the extra weight of the fluorescent tag and actin runs at ~45kDa.

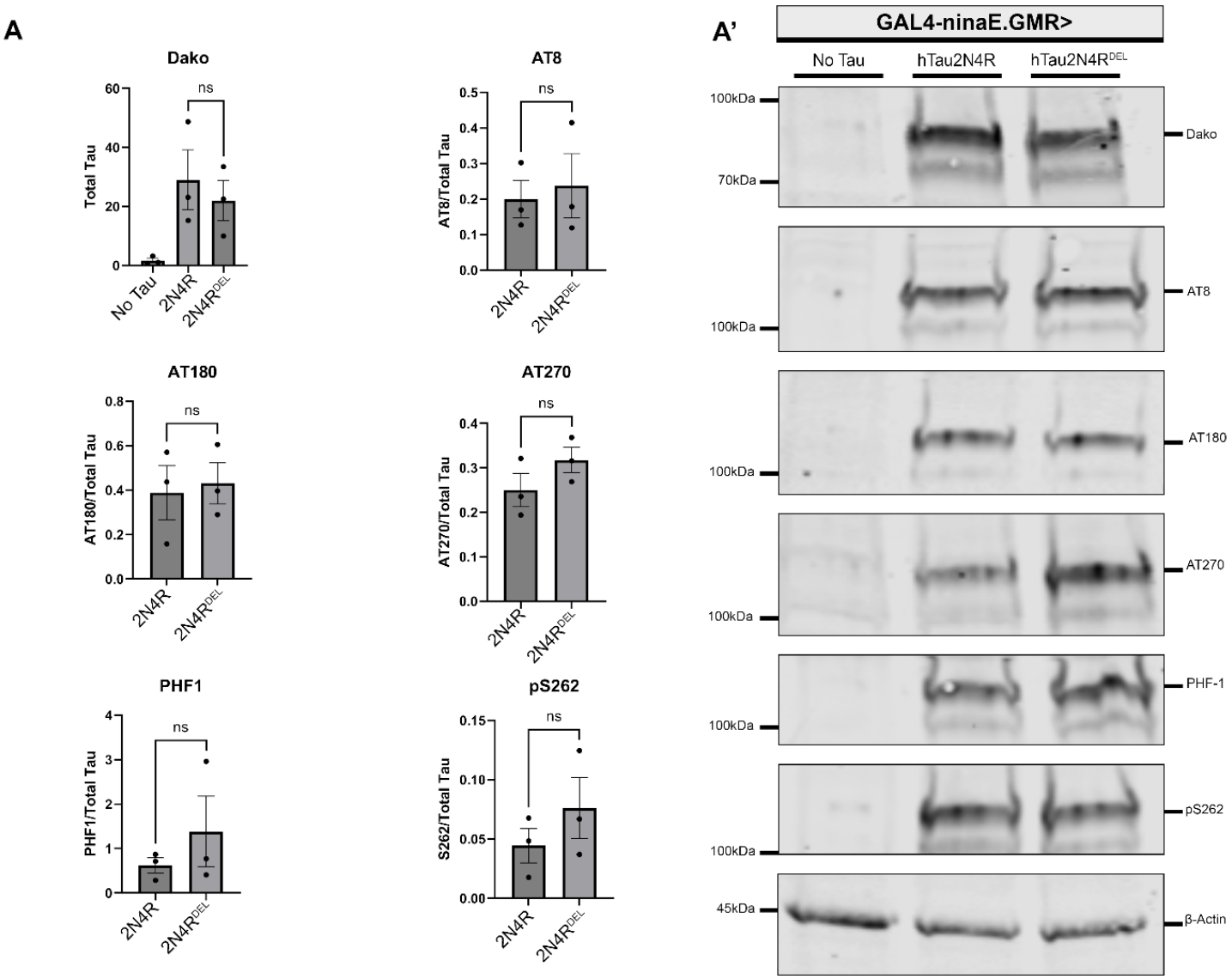

Supplementary Figure 9. All mutants bind to microtubules to the same extent.

A) Representative western blot and B) quantitative analysis of microtubule (MT)-bound Tau in 14-day-old male transgenic flies expressing Tau in adult retinal neurons using the GAL4-ninaE.GMR driver. Brain homogenates were fractioned into microtubule-bound (pellet) and unbound, free Tau (supernatant). mCherry::Tau constructs migrate to ~100kDa and α-Tubulin (loading control) migrates to ~50kDa. Error bars are plotted ±SD (N=3 biological repeats.). Statistical analysis was performed using a one-way ANOVA, and no statistical significance was reported between genotypes when *p<0.05.

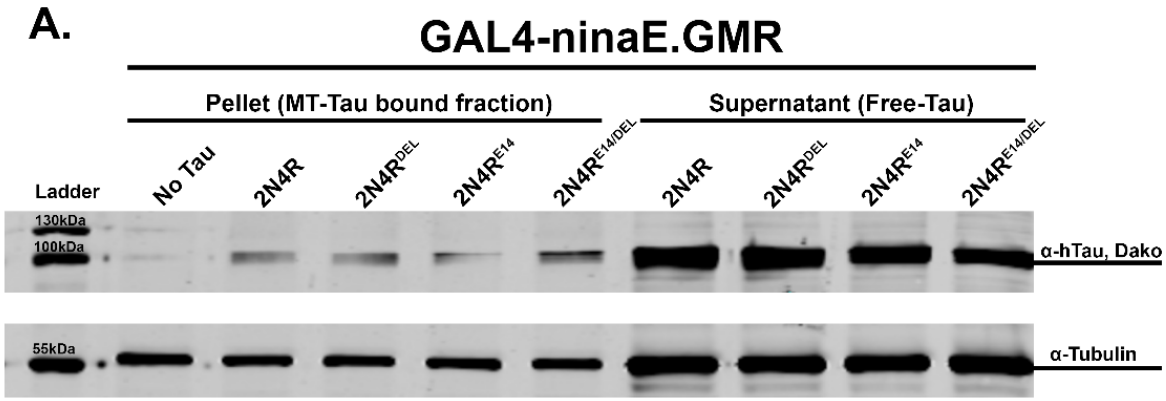

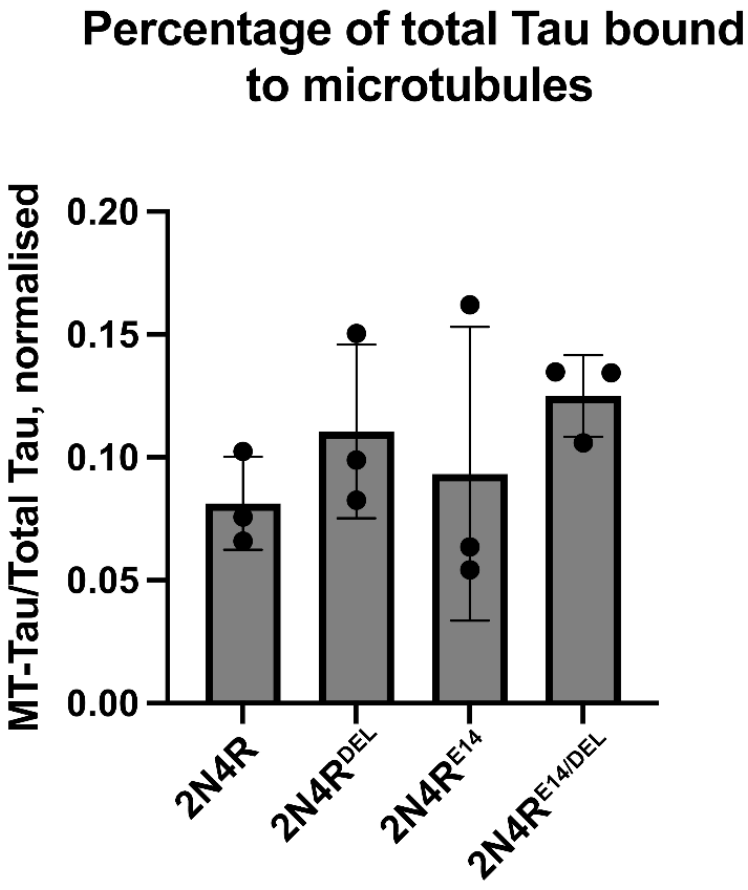

Supplementary Figure 10. ^{306}VQIVYK^{311} deletion rescues phosphorylation dependent production of pathogenic Tau conformations.

A) Maximum projection confocal images of the antennal lobe in the brain of 14-day-old flies expressing mCherry::Tau mutants in the Or47b neurons. Rows represent isolated channels 1) membrane bound CD8::GFP tagging the neuron morphology, 2) mCherry::Tau and 3)MC1 antibody detecting pathological misfolded conformations of Tau and 4) composite image of mCherry::Tau and MC1 to show the co-localisation of misfolded Tau within the total Tau expressed. Arrows indicate MC1-positive accumulations, which are substantially more abundant and extensive in hTau2N4R^{E14} neurons compared to all other genotypes. B) Quantification of misfolded Tau proportion within expressing neurons using MATLAB-based automated segmentation of GFP signal to distinguish neuron-specific (GFP-positive) from background (GFP-negative) pixels. Fluorescence values represent average MC1 signal within GFP-positive pixels minus background signal from GFP-negative pixels. hTau2N4R^{E14} shows significantly elevated misfolded Tau levels, which are rescued by ^{306}VQIVYK^{311} deletion in hTau2N4R$^{E14/DEL}$. Graphs represent mean ± SD (N=4 from single biological replicate). Statistical analysis: one-way ANOVA with Tukey's multiple comparisons (***p<0.001, ****p<0.0001).

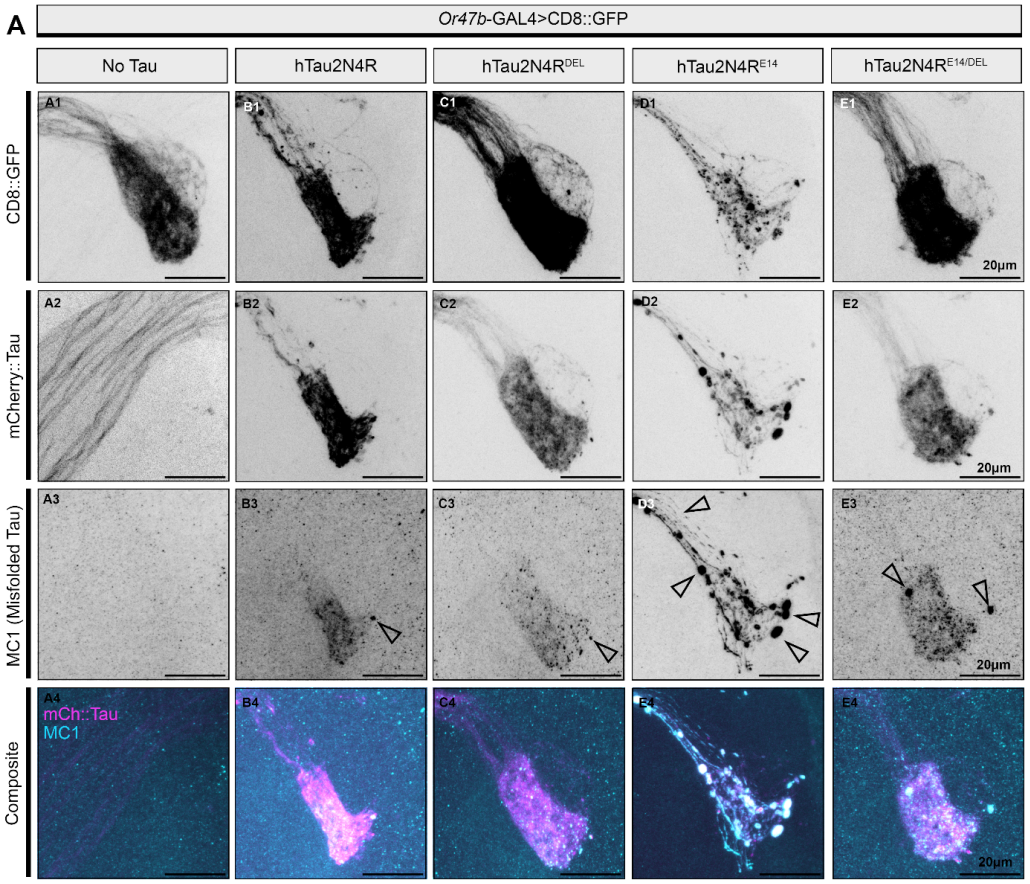

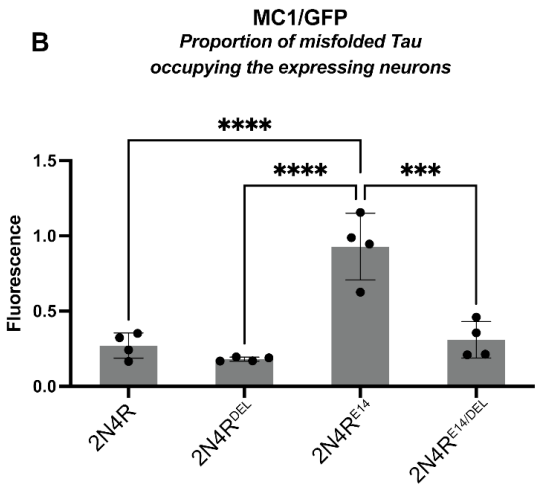

Supplementary Figure 11. Using IMARIS software for quantification of Tau accumulation and neuronal degeneration using "spots" and "surfaces" masking tools.